Growing season extension and its impact on terrestrial carbon cycle in the Northern Hemisphere over the past 2 decades

Shilong Piao, Pierre Friedlingstein, Philippe Ciais, Nicolas Viovy, Jérôme Demarty

Growing season extension and its impact on terrestrial carbon cycle in the Northern Hemisphere over the past 2 decades

Shilong Piao,[1] Pierre Friedlingstein,[1] Philippe Ciais,[1] Nicolas Viovy,[1] and Jérôme Demarty[1]

Received 9 November 2006; revised 29 May 2007; accepted 9 July 2007; published 25 September 2007.

[1] A number of studies have suggested that the growing season duration has significantly lengthened during the past decades, but the connections between phenology variability and the terrestrial carbon (C) cycle are far from clear. In this study, we used the "ORganizing Carbon and Hydrology In Dynamic Ecosystems" (ORCHIDEE) process based ecosystem model together with observed climate data to investigate spatiotemporal changes in phenology and their impacts on carbon fluxes in the Northern Hemisphere (>25°N) during 1980–2002. We found that the growing season length (GSL) has increased by 0.30 days yr^{-1} ($R^2 = 0.27$, $P = 0.010$), owing to the combination of an earlier onset in spring (0.16 days yr^{-1}) and a later termination in autumn (0.14 days yr^{-1}). Trends in the GSL are however highly variable across the regions. In Eurasia, there is a significant trend toward earlier vegetation green-up with an overall advancement rate of 0.28 days yr^{-1} ($R^2 = 0.32$, $P = 0.005$), while in North America there is a significantly delayed vegetation senescence by 0.28 days yr^{-1} ($R^2 = 0.26$, $P = 0.013$) during the study period. Our results also suggested that the GSL strongly correlates with annual gross primary productivity (GPP) and net primary productivity (NPP), indicating that longer growing seasons may eventually enhance vegetation growth. A 1-day extension in GSL leads to an increase in annual GPP of 5.8 gC m^{-2} yr^{-1} (or 0.6% per day), and an increase in NPP of 2.8 gC m^{-2} yr^{-1} per day. However, owing to enhanced soil carbon decomposition accompanying the GPP increase, a change in GSL correlates only poorly with a change in annual net ecosystem productivity (NEP).

Citation: Piao, S., P. Friedlingstein, P. Ciais, N. Viovy, and J. Demarty (2007), Growing season extension and its impact on terrestrial carbon cycle in the Northern Hemisphere over the past 2 decades, *Global Biogeochem. Cycles*, *21*, GB3018, doi:10.1029/2006GB002888.

1. Introduction

[2] Climate change has already affected the terrestrial ecosystems both structurally and functionally [*Walther et al.*, 2002]. An easily observable effect of such ongoing changes is the timing of phenology events, such as bud-burst, flowering, leaf unfolding, and leaf coloration [*Penuelas and Filella*, 2001]. Phenology studies based on field observations [*Menzel and Fabian*, 1999; *Ahas et al.*, 2000], remote sensing data [*Myneni et al.*, 1997; *Zhou et al.*, 2001; *Tucker et al.*, 2001; *Suzuki et al.*, 2003; *Stöckli and Vidale*, 2004], atmospheric CO_2 observation data [*Keeling et al.*, 1996], and ecological process modeling [*Lucht et al.*, 2002] all robustly indicate that the vegetation growing season length (GSL) significantly increased over the past decades, principally through an earlier beginning and a later termination.

[3] Interannual variability and trends in the timing and length of the growing season modifies biosphere-atmosphere interactions, and induces changes in albedo [*Chapin et al.*, 2005], in carbon [*Wilson and Baldocchi*, 2000; *Baldocchi et al.*, 2001; *White and Nemani*, 2003; *McDonald et al.*, 2004; *Niemand et al.*, 2005] and nutrient cycling [*Stockfors and Linder*, 1998]. Using a combination of biogeochemical and atmospheric modeling, *Randerson et al.* [1999] suggested that an increase in early season plant carbon uptake driven by warmer spring conditions can account for the observed enhanced amplitude and advanced timing of the seasonal cycle of atmospheric CO_2 concentration [*Keeling et al.*, 1996]. Therefore quantifying the effect of phenological variability on the terrestrial carbon cycle is necessary for understanding the mechanisms of the current trends of vegetation "greening" and carbon sinks observed in the middle and high latitudes of the Northern Hemisphere [*Zhou et al.*, 2001; *Nemani et al.*, 2003].

[4] Developments in the fields of eddy-covariance techniques and terrestrial ecosystem modeling have greatly increased the opportunity for exploring the potential effect of vegetation growing season extension on terrestrial carbon exchange with atmosphere. A recent study based on multi-year tower eddy flux measurements of CO_2 exchange and phenology over Tharandt Forest Anchor Station reported

[1]Laboratoire des Sciences du Climat et de l'Environnement, UMR CEA-CNRS, Gif-sur-Yvette, France.

0886-6236/07/2006GB002888

Table 1. PFTs and PFT-Specific Parameters of Phenology Submodel in ORCHIDEE[a]

		Green-Up			Vegetation Senescence		
PFT	Phenology Type	GDDg, °C*days	NGDg, days	Hg, days	Ac, days	Ts, °C	Hs
TrBE					910		
TrBR	moi			50	180		0.3
TeNE					910		
TeBE					730		
TeBS	ncdgdd	$603e^{-0.0091N} - 64$			180	12.5	
BoNE					910		
BoBS	ncdgdd	$603e^{-0.0091\ N} - 64$			180	5	
BoNS	ngd		17		180	7	
NC3	moigdd	185		35	120	4	0.2
NC4	moigdd	400		35	120	5	0.2
AC3	moigdd	125		75	150	10	0.2
AC4	moigdd	400		75	120	10	0.2

[a]The PFTs are: tropical broadleaf evergreen forests (TrBE), tropical broadleaf raingreen forests (TrBR), temperate needleleaf evergreen forests (TeNE), temperate broadleaf evergreen forests (TeBE), temperate broadleaf summergreen forests (TeBS), boreal needleleaf evergreen forests (BoNE), boreal broadleaf summergreen forests (BoBS), boreal needleleaf summergreen forest (BoNS), natural C_2 grass (NC3), natural C_4 grass (NC4), agriculture C_2 grass (AC3), and agriculture C_4 grass (AC4). Phenology types are: onset date of green-up dependent on soil moisture (moi), onset date of green-up dependent on growing degree days (ncdgdd), onset date of green-up dependent on number of growing days (ngd), and onset date of green-up dependent on growing degree days and soil moisture (moigdd). GDDg, critical growing degree days (°C*days); NGDg, critical number of growing days (days); Hg, minimum time elapsed since moisture minimum (days); Ac, critical leaf age for leaf senescence (days); Ts, critical weekly temperature for leaf senescence (°C); Hs, critical weekly moisture stress for leaf senescence; and N, number of chilling days.

that annual GPP for old coniferous forest dominated by Norway spruce increased by approximately 17 gC m^{-2} yr^{-1} with the extension of GSL [*Niemand et al.*, 2005]. According to global temperate forest flux measurements, an increase in annual NEP in response to extending the carbon uptake period for temperate broadleaf summergreen forest is around 5.7 gC m^{-2} yr^{-1} per day [*Baldocchi et al.*, 2001]. Modeling studies suggested that a 1-day extension of GSL is sufficient to lead to an increase of 0.5% in the annual GPP of deciduous forest [*White et al.*, 1999]. Similarly, the sensitivity of annual NPP to the timing of spring plant emergence was also found to be on the order of 1% per day for boreal forests [*Kimball et al.*, 2004].

[5] The primary objective of this study is to investigate the links between the trends of phenological events and terrestrial carbon fluxes at the global scale. To achieve this goal, we use a process based ecosystem model called ORCHIDEE. The model is forced on an hourly basis by observed climate and weather data to simulate carbon fluxes as well as the timing of phenological events. The model results, archived on a daily time step over the period 1980–2002 are analyzed for the changes in the onset and termination of the growing season, and their subsequent relationships with gross and net carbon fluxes at different scales.

2. Methods and Data Sets

2.1. Process-Based ORCHIDEE Model

[6] A recently developed dynamic global vegetation model called ORCHIDEE (''ORganizing Carbon and Hydrology In Dynamic Ecosystems'') was used to simulate terrestrial carbon dynamics as well as phenological events. The ORCHIDEE model is composed of three coupled submodels: a surface-vegetation-atmosphere transfer model SECHIBA [*Ducoudré et al.*, 1993], a biogeochemical process model STOMATE and a third model dealing with ecosystem dynamics (i.e., fire, sapling establishment, light competition, tree mortality). SECHIBA simulates on a half-hourly time step the processes of photosynthesis, energy and water exchanges between atmosphere and land, as well as the soil moisture budget. The onset and senescence of foliage development, and the flows of carbon within the ecosystem pools (i.e., carbon allocation, mortality, litter decomposition, and soil carbon decomposition) are calculated by the STOMATE submodel, at a daily time step.

[7] Several phenology models have been developed for various spatial scales and application purposes. The phenology model used in ORCHIDEE is process driven, and developed from satellite-derived phenological observation [*Botta et al.*, 2000]. The onset of leaf growth is generally triggered by parameters such as the number of growing degree days and chilling days, photoperiod, soil moisture contents, and vegetation type [*Moulin et al.*, 1997]. The global vegetation in ORCHIDEE is classified into 12 Plant Functional Types (PFT), which all have distinct phenological criteria (Table 1). Temperature is the principal trigger of growth onset for temperate and boreal vegetation. Accordingly, the green-up date of boreal needleleaf summergreen forests is estimated from a number of growing days, defined as the number of days over a given period for which the daily mean air temperature is above a threshold (i.e., −5°C). The effect of temperature on green-up for broadleaf summergreen forests is estimated on the basis of growing degree days (GDD), which further depends on the number of chilling days during the winter season. This number is calculated as the number of days from the moment when weekly NPP has fallen below 20% of last year's maximum weekly NPP to the moment when daily mean air temperature is below a particular threshold (−5°C for temperate broadleaf summergreen forests and 0°C for boreal broadleaf summergreen forests). For grasses, beginning of the growing season depends on both GDD and soil moisture availability. Generally, an increase in chilling days reduces the GDD demand of broadleaf summergreen forests as

$$g_c = 603 \times e^{-0.0091n} - 64, \quad (1)$$

where g_c is required GDD demand for leaf onset, n is number of chilling days.

[8] Leaf senescence depends on a critical leaf age, water and temperature stresses. For temperate and boreal summergreen forests, leaves will shed when temperature decrease (i.e., current weekly temperature are lower than average temperature of the previous month) and weekly temperature fall below a prescribed threshold (i.e., 12.5°C for broadleaf summergreen forests, 5°C for boreal broadleaf summergreen forests and 7°C for boreal needleleaf summergreen forests). For grasses, leaves will shed when weekly soil moisture stress is below 0.2, or when weekly temperature is

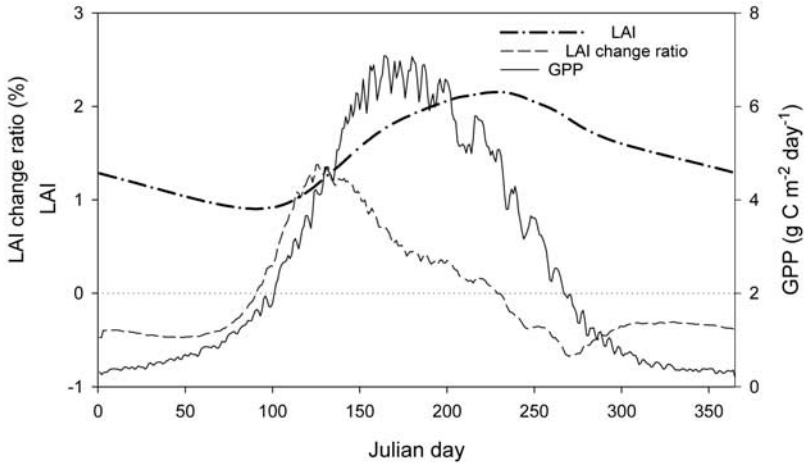

Figure 1. Seasonal variations in the 23-year averaged LAI and its change ratio as well as GPP for the entire study area. LAI change ration (LAI_{ratio}) is calculated using equation (3).

lower than 4°C. In addition, some fraction of the leaves is lost as a function of leaf age as

$$\Delta B_l = B_l \min\left(0.99, \frac{\Delta t}{a_c}\left(\frac{a}{a_c}\right)^4\right), \quad (2)$$

where a_c is the critical leaf age, B_l is leaf biomass at the time t, and a is the leaf age. Independent of PFT, critical leaf age is set from 6 months for natural grassland to 2.5 years for evergreen PFTs. Details of this model and parameters are described by *Krinner et al.* [2005] and *Botta et al.* [2000].

[9] *Botta et al.* [2000] calibrated their leaf onset model against satellite data, and derived realistic results for all PFT in the temperate and high latitudes; 62% of grid cells have a simulated date within 10 days of the satellite observed date (which is also the temporal resolution of remote sensing data). A general consistency was also found between the satellite-derived and modeled interannual variability of the onset date for each PFT during 1983–1993 [*Botta*, 1999]. The seasonal cycles of energy and water exchanges and carbon fluxes from ORCHIDEE model have also validated by comparing eddy covariance data at particular sites around the world, and found that the simulation results compare well with observation [*Krinner et al.*, 2005]. The model also realistically represents spatial distribution of vegetation and leaf density at global or regional scales [*Krinner et al.*, 2005].

2.2. Data Sets

[10] We run the ORCHIDEE model with observed climate and weather data and rising atmospheric CO_2, using prescribed actual vegetation and soil distribution information to quantify interannual changes in phenology and GPP, NPP, NEP. The meteorological data required as input for the ORCHIDEE model include air temperature, precipitation, wet day frequency, diurnal temperature range, cloud cover, relative humidity of the air and wind speed. Monthly data sets, with a spatial resolution of 0.5° for 1901–2002, were supplied by the Climatic Research Unit (CRU), School of Environmental Sciences, University of East Anglia, U.K. [*Mitchell and Jones*, 2005]. These data were transformed to daily weather variables using a weather generator [*Richardson and Wright*, 1984].

2.3. Simulation and Analysis

[11] Using 1901 climate data and the 1860 atmospheric CO_2 concentration of 286 ppm, we first run the model at a resolution of 2 degree until the carbon pools reach equilibrium (about 1000 years). Owing to a lack of climate data during the period of 1860–1900, the model is then run to 1900 with the climatology selected from a random sequence of years between 1901 and 1910 and atmospheric CO_2 concentration of the corresponding year. This state was used as an initial condition for the 1901–2002 run. The model results from 1980 to 2002 were saved at a daily time step and analyzed in the following.

[12] A "sudden change" in leaf stage can be related to the onset or cessation of "significant photosynthetic activity" [*Reed et al.*, 1994; *Moulin et al.*, 1997]. The two stages of the growing season, i.e., vegetation green-up and senescence, are calculated on the basis of the seasonal cycle of LAI (Figure 1). In general, for a biome at each pixel, its LAI value gradually increases first, reaches a maximum, and then decreases with increasing Julian day during the growing season. The onset time of vegetation green-up is defined as the day when LAI starts to increase. For the vegetation senescence, we first use the mean LAI seasonal cycle during 1980–2002 to calculate a LAI threshold corresponding to the inception of senescence when the highest negative relative LAI change, namely minimum value of LAI change ratio (LAI_{ratio}) (by equation (3)) occurs. However, if the highest negative relative LAI change occurs after the mean GPP upward crossed the zero axis, LAI value of mean GPP upward zero crossing time is calculated as the LAI threshold of the corresponding onset date of vegetation senescence. Then the onset date of vegetation senescence for each year is defined as the day when LAI value down crossed the

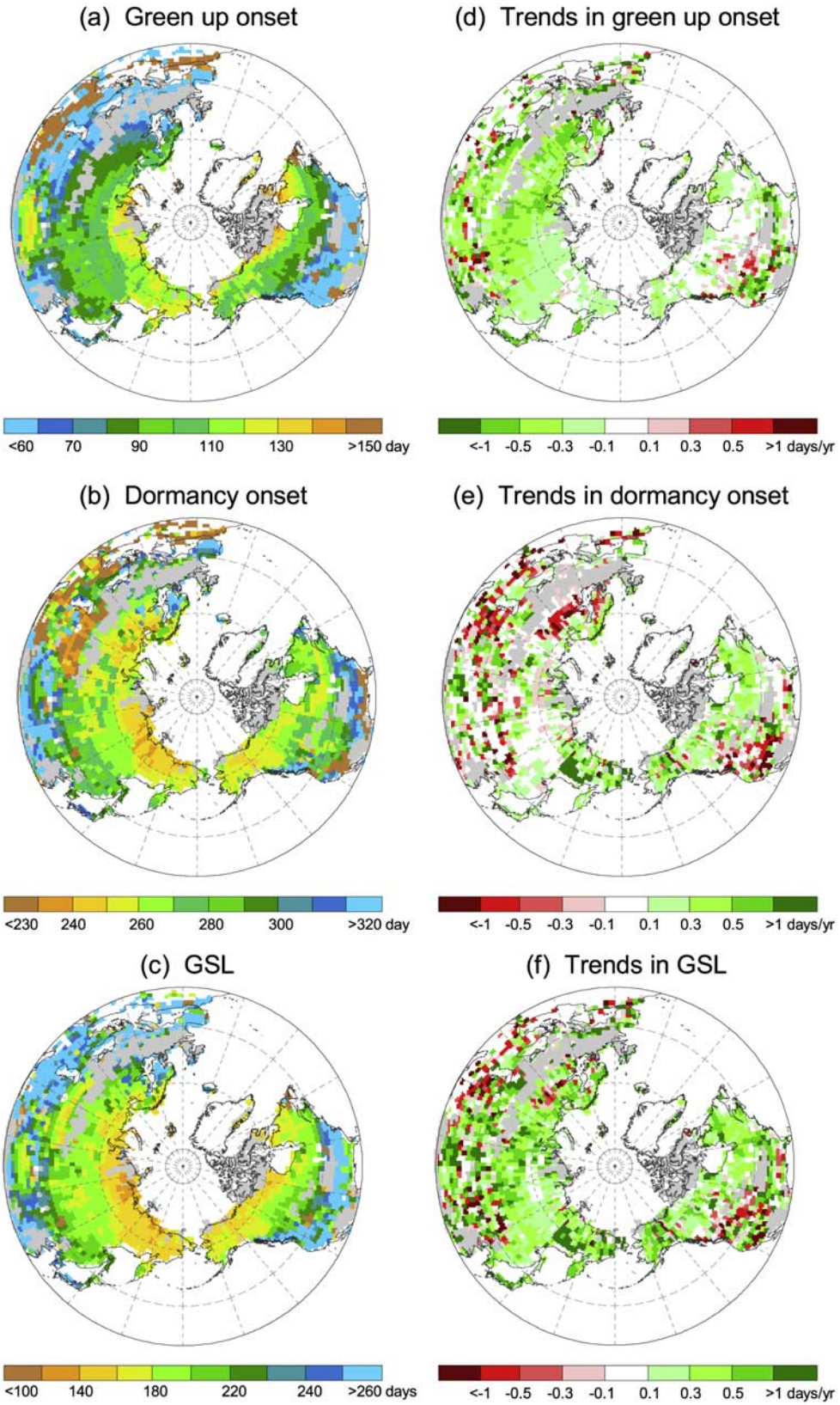
(a) Green up onset
<60 70 90 110 130 >150 day
(d) Trends in green up onset
<-1 -0.5 -0.3 -0.1 0.1 0.3 0.5 >1 days/yr
(b) Dormancy onset
<230 240 260 280 300 >320 day
(e) Trends in dormancy onset
<-1 -0.5 -0.3 -0.1 0.1 0.3 0.5 >1 days/yr
(c) GSL
<100 140 180 220 240 >260 days
(f) Trends in GSL
<-1 -0.5 -0.3 -0.1 0.1 0.3 0.5 >1 days/yr

Figure 2

thresholds. These onset dates were then used to analyze their trends over year.

$$LAI_{ratio}(t) = [LAI(t+1) - LAI(t)]/[LAI(t)] \times 100, \quad (3)$$

where t is time (temporal resolution of 1 day), and LAI(t) is LAI value at Julian day t. Since in this version of ORCHIDEE, crop phenology is simply treated in very similar manner to that of grassland, we only analyze grid cells with <50% fraction of crop.

3. Results

3.1. Mean Patterns

[13] The model-simulated seasonal variations in the 23-year averaged LAI and its change ratio (LAI_{ratio}) as well as GPP for the entire study area (>25°N) are shown in Figure 1. The LAI value starts to increase on Julian day 91 (1 April) and then decreases gradually after reaching its maximum on Julian day 229 (17 August). The minimum value of LAI_{ratio} occurs on Julian day 271 (28 September). Therefore we determined the Julian day 91 to be the mean onset date of green-up and Julian day 271 to be that of vegetation senescence for the entire study area.

[14] Figure 2a displays the spatial distribution of the mean onset dates of green-up as calculated from the ORCHIDEE model for the period 1980–2002. As expected, the mean green-up date is progressively delayed with increasing latitude and increasing continentality. The latest dates of green-up occur in northern Siberia, northern Canada, and over the Tibetan Plateau, owing to low temperatures. It should be noted that in Mediterranean regions, such as Spain and North Africa, the vegetation cycle begins in the fall, coincidently with an increase in precipitation and soil moisture content [*Moulin et al.*, 1997]. The dates of vegetation senescence, shown in Figure 2b occur in reverse order of the green-up onset. In particular, Southwestern Eurasia has the earliest senescence dates. Grasses and crops prevail over that region, where precipitation in late summer is relatively low. As a consequence of this heat and water stress, LAI decreases rapidly by late summer, and senescence occurs in August. The GSL, shown in Figure 2c, is found to increase dramatically with decreasing latitude. It is the shortest in central and eastern Siberia along the Arctic coast, with a duration of only 3 months. In contrast, most of Europe, Eastern China and Southern North America have long growing seasons, lasting up to 8 months.

3.2. Trends in Phenology

3.2.1. Trends Over the Entire Study Area

[15] Between 1980 and 2002, the mean dates of vegetation green-up have advanced at a fast rate of 0.16 days yr^{-1} ($R^2 = 0.23$, $P = 0.021$) over the study area (Figure 3a). Such a spring phenology trend is caused by a significant increase in spring temperature. The mean temperature in March–April over the study area has increased by 0.06°C yr^{-1} ($R^2 = 0.35$, $P = 0.003$) during the past two decades. Regression analysis indicates that over northern ecosystems, the warming trend of spring temperature triggers an earlier vegetation green-up of 3.0 days $°C^{-1}$ ($R^2 = 0.76$, $P < 0.001$).

[16] The mean onset date of vegetation senescence shows a dramatic delay of 0.14 days yr^{-1} over the 23 years ($R^2 = 0.18$, $P = 0.043$), coincident with the mean autumn (September and October) temperature change of 0.031°C yr^{-1} ($R^2 = 0.27$, $P = 0.011$) (Figure 3b). An increase in mean autumn temperature by 1°C delays the vegetation senescence by 3.1 days ($R^2 = 0.31$, $P = 0.006$). Overall, the GSL north of 25°N has lengthened by on average 0.30 days yr^{-1} since 1980 ($R^2 = 0.27$, $P = 0.010$).

3.2.2. Spatial Patterns of Trends

[17] Linear trends in vegetation green-up dates and GSL over 1980–2002 were computed in each pixel using linear regression analysis according to the equation of onset timing of spring (dependent variable) with year (independent variables). The spatial patterns of the trends in vegetation green-up are mapped in Figure 2d. More than 70% of the study region experienced an advancing trend in the vegetation green-up, due to increasing spring temperature. The largest advancement in green-up (over 0.5 days yr^{-1}) mainly occurs in southern Siberia, eastern China, Europe and southeastern and south western North America. In Europe and East Asia, recent analysis based on multiyear remote sensing data have also found a significant trend toward advanced onset dates of vegetation green-up with rates of 0.54 days yr^{-1} and 0.79 days yr^{-1}, respectively [*Stöckli and Vidale*, 2004; Piao et al., 2006a]. In addition, according to *Chmielewski and Rotzer* [2001], the average leaf unfolding of four tree species in Europe advanced by 8 days from 1989 to 1998. In western USA, bloom dates occurred 5–10 days earlier since the late 1970s [*Cayan et al.*, 2001].

[18] Previous studies have suggested that later onset of autumnal phenological events are less pronounced and show a more heterogeneous pattern than spring phenological events [*Walther et al.*, 2002]. The model simulated trends in the onset of senescence also exhibit a more fragmented pattern (Figure 2e). While some regions in south western North America experienced an earlier termination of the growing season, most of northern North America (>50°N) shows a trend toward later growing season end. In Eurasia, the regions showing a trend toward an earlier senescence are the Caspian Sea and Eastern Europe. Such spatial heterogeneity of trends in onset of senescence may result mainly from differences in regional climate changes. In Eastern Europe, this trend is coupled with decreasing autumn temperature [*Intergovernmental Panel on Climate Change*, 2001], whereas in southwestern

Figure 2. Spatial distribution of ORCHIDEE model-derived onset timing of vegetation green-up, vegetation senescence, and length of growing season for all areas of north of 25°N. (a) Average Julian day of vegetation green-up, (b) average Julian day of vegetation senescence, (c) average growing season length, (d) trends in dates of vegetation green-up (days yr^{-1}), (e) trends in dates of vegetation senescence (days yr^{-1}), and (f) trends in growing season length (days yr^{-1}). Grid cells with >50% of crop fraction and spare vegetation cover are shown masked in gray.

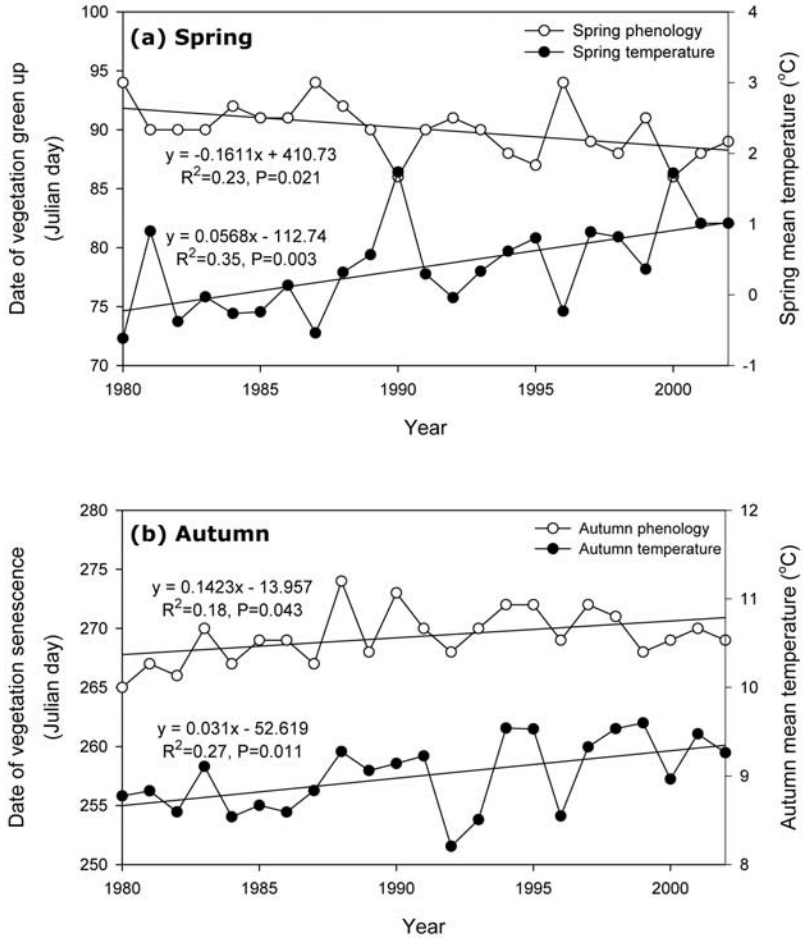

Figure 3. Interannual changes in (a) dates of vegetation green-up and spring temperature and (b) dates of vegetation senescence and autumn temperature for entire study area from 1980 to 2002.

North America and the Caspian Sea regions, it may be associated with the heat or water stress induced by regional warming [*Angert et al.*, 2005].

[19] There is some spatial heterogeneity in the spatial distribution of the GSL trends shown in Figure 2f. North of approx. 55°N, the average GSL is modeled to increase, usually as a combined result of earlier green-up in Eurasia and later senescence in North America. Areas characterized by a decline in the GSL are located mainly between 30°N and 50°N in central and western United States, and in Central Asia.

[20] Table 2 compares the trends in the timing of the growing season during the past 23 years between Eurasia and North America. In Eurasia, there is a significant trend toward earlier vegetation green-up with an overall advancement rate of 0.28 days yr^{-1} ($R^2 = 0.32$, $P = 0.005$). In stark contrast, the green-up dates over North America do not show any statistically significant trend ($R^2 = 0.00$, $P = 0.923$). On

Table 2. Linear Trends (days yr^{-1}) and Level of Statistical Significance (P) in Onset Timing of Phenology Events and Growing Season Length (GSL) for Different Regions From 1980 to 2002

		Green-Up		Vegetation Senescence		GSL	
Region	Latitude	Trend, days yr^{-1}	P	Trend, days yr^{-1}	P	Trend, days yr^{-1}	P
Eurasia	25°N–50°N	−0.41	0.016	0.02	0.904	0.43	0.055
	50°N–90°N	−0.28	0.021	0.12	0.159	0.40	0.023
	25°N–90°N	−0.28	0.005	0.11	0.238	0.39	0.013
North America	25°N–50°N	−0.01	0.979	0.12	0.361	0.13	0.725
	50°N–90°N	−0.07	0.541	0.50	0.003	0.56	0.009
	25°N–90°N	−0.01	0.923	0.28	0.013	0.29	0.048

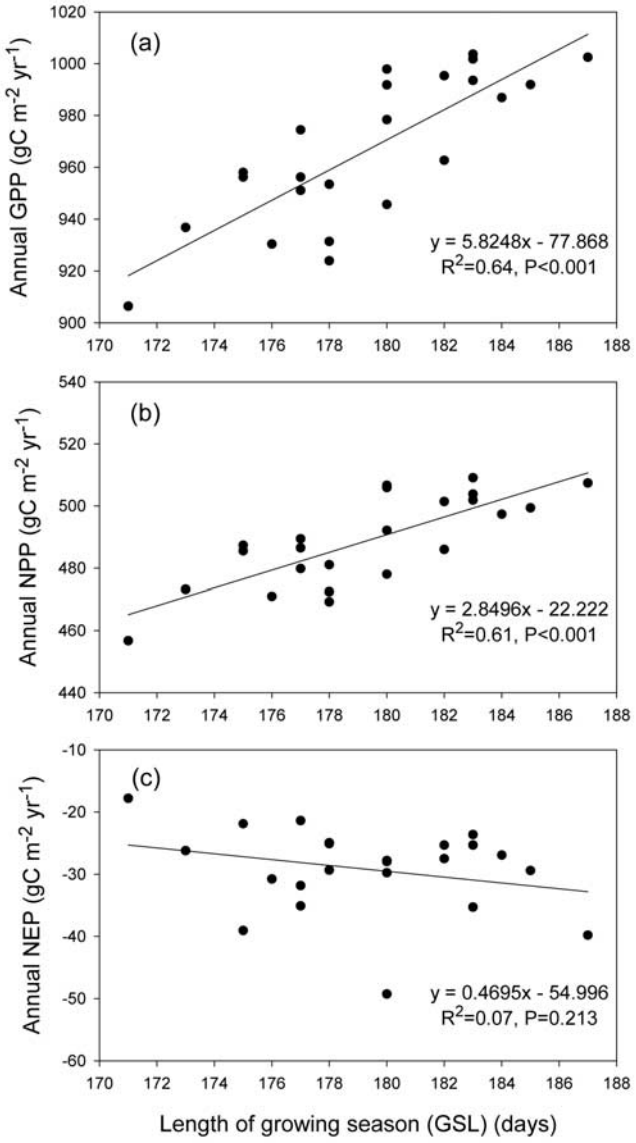

Figure 4. Relationships between (a) growing season length and annual GPP, (b) growing season length and annual NPP, and (c) growing season length and annual NEP for entire study area.

the other hand, North America exhibits significantly delayed vegetation senescence (R^2 = 0.26, P = 0.013), especially at high latitudes (>50°N) where the dates of vegetation senescence have changed by 0.50 days yr^{-1} (R^2 = 0.34, P = 0.003).

3.3. Correlation Between Carbon Fluxes and Growing Season Length

[21] We performed a temporal correlation analysis between the growing season length and the component carbon fluxes of GPP, NPP and NEP. The results indicate that the GSL closely and positively correlates with annual GPP (R^2 = 0.64, P < 0.001) and with annual NPP (R^2 = 0.61, P < 0.001), but not with NEP (R^2 = 0.07, P = 0.213) (Figure 4). This suggests that GSL can be a good predictor of annual GPP and NPP, but not of the net carbon balance of ecosystems. Regression analysis also shows that at the continental scale, lengthening of the growing season will cause an increase in GPP of 5.8 gC m^{-2} yr^{-1} per day (or 0.6% per day) and an increase in NPP of about half that amount (2.8 gC m^{-2} yr^{-1} per day).

[22] We further regressed GSL with carbon fluxes for temperate and boreal PFTs (Table 3). Since ORCHIDEE does only calculate soil respiration on a grid cell and not for each PFT present in the same grid cell, we only characterized the linear regression slope of GSL versus GPP and NPP. For more than 80% of all grid points containing the considered PFTs, we found a significant positive correlation between annual GPP and GSL. The largest slope corresponds to temperate broadleaf summergreen forests (9.8±2.6 gC m^{-2} yr^{-1} per day), which could probably be attributed to its relatively high GPP adjusted for the length of growing season (the ratio of annual GPP to GSL) as observed by eddy covariance measurements. Both our modeling simulation and independent analysis of eddy covariance measurements by *Falge et al.* [2002] show that temperate broadleaf summergreen forest have the largest GPP adjusted for the GSL among the above all biomes, i.e., 9.0 gC m^{-2} per day and 8.3 gC m^{-2} per day, respectively. Boreal needleleaf summergreen forests tend to show a largest relative increase rate of GPP associated with GSL (0.8 ± 0.4% per day) as seen in Table 3. Similarly, annual NPP for each PFT is also positively correlated with GSL. The different slope between the GPP and the NPP regression is due to concurrent changes in vegetation autotrophic respiration.

[23] Since ORCHIDEE model does not provide soil respiration for each biome type, we only selected pixels that are "pure" in terms of biome type (i.e., a pixel need to have over 90% of temperate broadleaf summergreen forest area to be a "temperate broadleaf summergreen forest" pixel) to investigate the relationships between NEP and GSL for each biome. All biome show that GSL is not significantly correlated with annual NEP in more than 50% of grid points containing the considered PFTs, indicating that extending GSL does not necessarily lead to higher net CO_2 uptake.

4. Discussion

4.1. Phenology Changes

[24] Advanced beginning of spring and/or postponed ending of autumn seasons have been widely reported across the world in recent phenological studies [*Menzel and Fabian*, 1999; *Ahas et al.*, 2000; *Myneni et al.*, 1997; *Zhou et al.*, 2001; *Tucker et al.*, 2001; *McDonald et al.*, 2004; *Smith et al.*, 2004; *Linderholm*, 2006]. A new finding revealed in this study is that trends in the onset dates of vegetation green-up at the continental scale are substantially different between North America and Eurasia. In Eurasia, there is a significant trend toward earlier beginning of growing season by 0.28 days yr^{-1} (R^2 = 0.32, P = 0.005), whereas the beginning of growing season in North America does not show statistically significant trends (0.01 days

Table 3. Summary of Relationships Between Annual C Flux and Length of Growing Season for Different Biomes[a]

	GPP Versus GSL			NPP Versus GSL			NEP Versus GSL	
Biome	S, gC m^{-2} yr^{-1} day^{-1}	Re, % day^{-1}	N, %	S, gC m^{-2} yr^{-1} day^{-1}	Re, % day^{-1}	N, %	S, gC m^{-2} yr^{-1} day^{-1}	N, %
TeBS	9.8 ± 2.6	0.6 ± 0.3	96.7	4.8 ± 1.8	0.5 ± 0.3	90.2	1.9 ± 1.6	26.2
BoNS	6.1 ± 1.7	0.8 ± 0.4	99.7	3.4 ± 1.1	0.8 ± 0.4	99.4	1.1 ± 1.0	10.5
BoNE	4.9 ± 2.5	0.4 ± 0.2	91.2	2.2 ± 1.1	0.4 ± 0.2	91.5		
TG	3.7 ± 2.4	0.5 ± 0.4	85.5	2.0 ± 1.2	0.5 ± 0.4	85.1	0.3 ± 1.2	5.4
Tundra	6.2 ± 5.0	0.7 ± 0.5	87.7	3.5 ± 2.7	0.6 ± 0.4	86.1	1.0 ± 0.8	46.3

[a]Only pixels that are "pure" in terms of biome type (i.e., a pixel need to have over 90% of temperate broadleaf summergreen forest area to be a "temperate broadleaf summergreen forest" pixel) to investigate the relationships between net ecosystem productivity (NEP) and growing season length (GSL) for each biome. There are no pixels with more than 90% fraction of boreal needleleaf evergreen forest. S, magnitude of changes in annual C flux for every one-day extension of GSL (gC m^{-2} yr^{-1} per day); Re, relative changes in annual C flux for every one-day extension of GSL (% per day); N, fraction of number of pixels with significant correlation between C flux and GSL at 0.05 significance level to total numbers for each biome (%);TeBS, temperate broadleaf summer green forest; BoNS, boreal needleleaf summer green forest; BoNE, boreal needleleaf evergreen forest; TG, temperate grassland (multiannual mean temperature T > 10°C).

yr^{-1}, $R^2 = 0.00$, $P = 0.923$). This trend is comparable to the satellite-observed trends in the date of freeze-thaw. Using satellite data from the Scanning Multichannel Microwave Radiometer (SMMR) and Special Sensor Microwave/Imager (SSM/I), *Smith et al.* [2004] detected a trend of 0.39 days yr^{-1} toward earlier freeze-thaw in boreal Eurasia but only 0.08 days yr^{-1} in boreal North America (>45°N) during 1988–2002. In addition, LAI satellite products from the Global Inventory Monitoring and Modeling Studies (GIMMS) [*Tucker et al.*, 2005] also indicate that LAI has significantly increased in Eurasia ($R^2 = 0.37$, $P = 0.003$), but not in North America during the 1982–2002 period ($R^2 = 0.01$, $P = 0.622$). In contrast, *Zhou et al.* [2001] estimated similar advance of the growing seasons for Eurasia (0.3 days yr^{-1}) and North America (0.4 days yr^{-1}) during the 1981–1999 period.

[25] In autumn (September and October), however, the increase of LAI is larger in North America (0.005 yr^{-1}, $R^2 = 0.17$, $P = 0.063$) than that in Eurasia (0.003 yr^{-1}, $R^2 = 0.10$, $P = 0.156$). Similarly, smaller postponed trend of vegetation senescence date in Eurasia (0.11 days yr^{-1}) than in North America (0.28 days yr^{-1}) is found from our simulation. Although our modeled termination of the growing season in North America yields similar delayed trends (0.28 days yr^{-1}) as that derived from NOAA/AVHRR satellite data (0.21 days yr^{-1}) [*Zhou et al.*, 2001], the trends in Eurasia (0.11 days yr^{-1}) are much smaller than those of Zhou et al. (0.58 days yr^{-1}). Using the different method with that of *Zhou et al.* [2001], another estimation derived from NOAA/AVHRR satellite observations, however, showed earlier onset of autumn in Eurasia in both the 1980s and 1990s [*Tucker et al.*, 2001]. In addition, *Smith et al.* [2004] found a 0.31 days yr^{-1} trend toward earlier fall freezing in Eurasia. Such different results not only suggest large uncertainties in the estimation of current vegetation growing season changes at large scales, but also imply that the magnitude of phenological trends may vary dramatically with different definitions of growing season, period of investigation, and spatial scales [*Linderholm*, 2006]. *Walther and Linderholm* [2006] compared a number of definitions of growing season, and found that depending on the definition, GSL trends are very different. It should be noted that the model estimates the timing of photosynthesis cessation rather than leaf color change, which is visible from satellite images.

[26] Several factors, such as disease, competition, soil factors, and weather conditions, can profoundly influence plant phenological status. Among these factors, climate change, particularly the global warming, has been suggested to be the major cause of the advance and extension of the growing season [*Linderholm*, 2006]. Temperature change related interannual variation in phenology can be seen in Figure 3. For example, in 1980, 1987, 1992 and 1996, spring temperatures were abnormally low, coinciding with later onset dates of vegetation green-up (Figure 3a). Our result also suggest that over the northern ecosystems, the warming trend of spring temperature triggers an earlier vegetation green-up of 3 days $°C^{-1}$, which is close to the previous estimate of 4.0 days $°C^{-1}$ [*Fitter and Fitter*, 2002]. In addition, the different patterns of phenology change between North America and Eurasia may be attributed to different seasonal temperature changes between these two continents. The climate data show that spring (March and April) warming in North America ($R^2 = 0.04$, $P = 0.358$) is not as significant as autumn (September and October) warming ($R^2 = 0.27$, $P = 0.012$). Also, the reversed scenario is seen in Eurasia, where the mean spring warming trend of 0.07°C yr^{-1} ($R^2 = 0.32$, $P = 0.005$) is twice as large as the autumn warming trend (0.03°C yr^{-1}, $R^2 = 0.19$, $P = 0.038$) since 1980.

4.2. Effects of GSL Change on the Vegetation Productivity

[27] Several studies suggest that global warming as well as rising atmospheric CO_2 is a main driving force for the observed increase in vegetation productivity at middle and high latitudes of the Northern Hemisphere [*Korner*, 2000; *Zhou et al.*, 2001; *Lucht et al.*, 2002; *Piao et al.*, 2006b]. Generally the warming signal can influence productivity in two manners [*Wan et al.*, 2005]. One is the direct impact of rising temperatures on plant photosynthesis and growth. The other is the indirect impact due to changing phenology [*Fang et al.*, 2003], increasing soil nitrogen mineralization and availability [*Melillo et al.*, 2002], and reducing soil water content [*Wan et al.*, 2002]. In order to further separate the effects of longer GSL on vegetation productivity from

other factors mentioned above, we performed a multivariate regression analysis using annual C flux (GPP or NPP) as dependent variable and annual mean temperature (AT) and GSL as independent variables. The results show that both GSL and AT are significantly and positively correlated with annual GPP ($R^2_{GPP\text{-}GSL.\ AT} = 0.40$, $P = 0.002$; $R^2_{GPP\text{-}AT.\ GSL} = 0.25$, $P = 0.02$, respectively). While statistically controlling GSL, annual NPP is insignificantly correlated with AT ($R^2_{NPP\text{-}AT.\ GSL} = 0.11$, $P = 0.132$). However, there is still a significant correlation between annual NPP and GSL ($R^2_{NPP\text{-}GSL.\ AT} = 0.36$, $P = 0.003$). This suggests that a change in phenology is one of the most important factors affecting future vegetation productivity potential of northern terrestrial ecosystems with rising global temperature.

[28] The lengthening of vegetation growing season duration has been suggested to primarily account for the enhanced vegetation productivity observed in northern ecosystems over the past two decades [*Myneni et al.*, 1997; *Fang et al.*, 2003; *Nemani et al.*, 2003]. Indeed, our results show a meaningful impact of increase in GSL on the vegetation productivity at the global scale although such impact differed among biome types. Over the entire study area, the NPP increase in response to longer GSL is approximately 0.6% per day. Multiplying this average ratio by the growing season extension determined either from our phenological model (0.39 days yr^{-1} in Eurasia and 0.29 days yr^{-1} in North America) or from the NOAA/AVHRR NDVI data (0.97 days yr^{-1} in Eurasia and 0.64 days yr^{-1} in North America), one can predict that the annual NPP actually increased by 0.3–0.6% yr^{-1} in Eurasia and by 0.2–0.4% yr^{-1} in North America, approximating our estimation of 0.4% yr^{-1} in Eurasia and 0.3% yr^{-1} in North America over the study period. This increase is comparable to the one reported from remote sensing data analysis using empirical light-use efficiency models, i.e., 0.47% yr^{-1} in North America [*Hicke et al.*, 2002], 1.03% yr^{-1} in China [*Fang et al.*, 2003] and 0.34% yr^{-1} globally [*Nemani et al.*, 2003]. Similarly, our results suggest that terrestrial NPP over the study area increased at a rate of 0.35% yr^{-1} during the period 1980–2002 ($R^2 = 0.64$, $P < 0.001$).

[29] Our results also showed that there are noticeable effects of GSL on vegetation carbon storage. For each day that growing season increased over the entire study area, vegetation carbon storage increased by 8.5 gC m^{-2} ($R^2 = 0.35$, $P = 0.003$), which is similar to the TEM model estimates of 8.9 gC m^{-2} [*Euskirchen et al.*, 2006]. This finding indicates that recent extending of GSL as well as changes in land use [*Goodale et al.*, 2002] have resulted in an increase of terrestrial biomass storage in Northern Hemisphere. However, we could not determine the relative contribution of these two factors, because we did not take into account changes in land use in this study. Furthermore, there are also significant relationships between GSL and annual maximum LAI, which supports the results of *Myneni et al.* [1997] that extending growing season leads to an increase in annual maximum vegetation activity.

4.3. Effects of GSL Change on the NEP

[30] As well as NPP, heterotrophic respiration also affects net carbon exchange between atmosphere and terrestrial (NEP). The balance of these two major fluxes determines whether terrestrial ecosystems will act as a net C sink or source under climate changes. Although a decadal increase in GSL can profoundly enhance the carbon uptake by ecosystems, we found that the annual NEP did not systematically increase along with a longer GSL. This agrees with the results of recent analysis based on observing multiyear continuous in situ data at the Harvard Forest eddy-covariance site and biogeochemical modeling [*White and Nemani*, 2003]. The weak relationships between annual NEP and GSL could be explained by the opposing effect of enhanced soil carbon decomposition directly induced by warming which is suggested to be the major driving force of the extension of growing season [*Menzel and Fabian*, 1999; *Penuelas and Filella*, 2001]. Statistical analysis shows that approximately 0.5% (or 2.4 gC m^{-2} yr^{-1} per day) of annual heterotrophic respiration increased with a 1-day extension in GSL ($R^2 = 0.52$, $P < 0.001$). This result indicates that the connection between GSL and annual NEP is more complicated. Continuous eddy-covariance measurement should provide further opportunities to evaluate these relationships over longer time periods.

[31] Owing to lack of measurements on the state of canopy each day, carbon uptake period (defined as the period of terrestrial net carbon uptake from atmosphere, CUP) instead of GSL was widely used in previous eddy-covariance studies [*Baldocchi et al.*, 2001, 2005]. For example, *Baldocchi et al.* [2001] found a strong relationship between CUP and annual NEP across many temperate broadleaf summergreen forest sites from FLUXNET network, and suggested that extending GSL may induce an increase in terrestrial carbon sink. Recent analysis revealed that annual NEP is significantly correlated with CUP, but not with GSL [*White and Nemani*, 2003]. To test this hypothesis, we further examined the relationships between CUP and annual NEP for the entire study area (>25°N). The length of CUP was estimated from the dates when 5-day moving average of NEP crossed the zero axis in spring and again in autumn. We found a strong positive correlation between annual NEP and CUP ($R^2 = 0.56$, $P < 0.001$), comparing to a week correlation between annual NEP and GSL ($R^2 = 0.07$, $P = 0.213$). This suggests that CUP and GSL should not be equated.

5. Conclusions

[32] Using a process oriented ecosystem carbon model which calculates the growing season onset and termination as forced by climate and biogeochemical processes, we investigated interannual variability and decadal trends in phenology and their effects on terrestrial carbon cycling in the Northern Hemisphere from 1980 to 2002. Over most ecosystems north of 25°N, we modeled a trend toward longer growing seasons, usually caused by an earlier spring green-up in Eurasia and by a later senescence in North America. This result is in good general agreement with literature reports of lengthening growing seasons and ''greening trends'' in the Northern Hemisphere. Our model simulations also suggest that there is a significant positive correlation between annual GPP and NPP and growing

season duration, as observed at many eddy-covariance sites. This finding implies that the recent lengthening of the growing season as driven by warmer temperatures can strongly enhance plant growth and increase NPP over northern ecosystems. The pertaining NPP increase is sufficiently large to explain the current satellite observed trends in vegetation activity at middle and high latitudes, a result which points out to the key importance of phenological processes in controlling the vegetation productivity of northern ecosystems in response to future warming.

[33] Our modeling results also show that because of the contribution from concurrent stimulating of soil deposition, annual NEP does not exhibited significant correlation with GSL. Thus current extending GSL does not necessarily lead to increase in the magnitude of terrestrial carbon sink of Northern Hemisphere. More detailed studies based on long-term eddy-covariance data sets are needed to better understand the implications of growing season change for terrestrial net carbon gain.

[34] **Acknowledgments.** The authors wish to thank L. M. Zhou, J. Y. Fang, and N. de Noblet for helpful comments and discussions. The authors also acknowledge the useful comments provided by two anonymous reviewers. This study was supported by European community funded projects ENSEMBLES under contract GOCE-CT-2003-505539 and CARBOEUROPE IP programme. The computer time was provided by CEA.

References

Ahas, R., J. Jaagus, and A. Aasa (2000), The phenological calendar of Estonia and its correlation with mean air temperature, *Int. J. Biometeorol.*, *44*, 159–166.

Angert, A., et al. (2005), Drier summers cancel out the CO_2 uptake enhancement induced by warmer springs, *Proc. Natl. Acad. Sci. U. S. A.*, *102*, 10,823–10,827.

Baldocchi, D. D., E. Falge, and L. Gu (2001), FLUXNET: A new tool to study the temporal and spatial variability of ecosystem-scale carbon dioxide, water vapor, and energy flux densities, *Bull. Am. Meteorol. Soc.*, *82*, 2415–2433.

Baldocchi, D. D., et al. (2005), Predicting the onset of net carbon uptake by deciduous forests with soil temperature and climate data: a synthesis of FLUXNET data, *Int. J. Biometeorol.*, *49*, 377–387.

Botta, A. (1999), Modélisation globale de la ph énologie de la biosphére continentale à partir de données satellitaires, Ph.D. thesis, Univ. Pierre et Marie Curie, Paris.

Botta, A., N. Viovy, P. Ciais, and P. Friedlingstein (2000), A global prognostic scheme of leaf onset using satellite data, *Global Change Biol.*, *6*, 709–725.

Cayan, D., et al. (2001), Changes in the onset of spring in the western United States, *Bull. Am. Meteorol. Soc.*, *82*, 399–415.

Chapin, F. S., et al. (2005), Role of land-surface changes in Arctic summer warming, *Science*, *310*, 657–660.

Chmielewski, F. M., and T. Rotzer (2001), Response of tree phenology to climate change across Europe, *Agric. For. Meteorol.*, *108*, 101–112.

Ducoudré, N. I., K. Laval, and A. Perrier (1993), SECHIBA, a new set of parameterizations of the hydrologic exchanges at the land-atmosphere interface within the LMD atmospheric general circulation model, *J. Clim.*, *6*, 248–273.

Euskirchen, E. S., et al. (2006), Importance of recent shifts in soil thermal dynamics on growing season length, productivity, and carbon sequestration in terrestrial high-latitude ecosystems, *Global Change Biol.*, *12*, 731–750.

Falge, E., et al. (2002), Seasonality of ecosystem respiration and gross primary production as derived from FLUXNET measurements, *Agric. For. Meteorol.*, *113*, 53–74.

Fang, J. Y., et al. (2003), Increasing net primary production in China from 1982 to 1999, *Front. Ecol. Environ.*, *1*, 293–297.

Fitter, A. H., and R. S. R. Fitter (2002), Rapid changes in flowering time in British plants, *Science*, *296*, 1689–1691.

Goodale, C. L., et al. (2002), Forest carbon sinks in the Northern Hemisphere, *Ecol. Appl.*, *12*, 891–899.

Hicke, J. A., et al. (2002), Satellite-derived increases in net primary productivity across North America, 1982–1998, *Geophys. Res. Lett.*, *29*(10), 1427, doi:10.1029/2001GL013578.

Intergovernmental Panel on Climate Change (2001), *Climate Change 2001: Impacts, Adaptation, and Vulnerability: Contribution of Working Group II to the Third Assessment Report of the Intergovernmental Panel on Climate Change*, 1032 pp., Cambridge Univ. Press, Cambridge, U. K.

Keeling, C. D., J. F. S. Chin, and T. P. Whorf (1996), Increased activity of northern vegetation in inferred from atmospheric CO_2 measurements, *Nature*, *382*, 146–149.

Kimball, J. S., K. C. McDonald, S. W. Running, and S. E. Frolking (2004), Satellite radar remote sensing of seasonal growing seasons for boreal and sub-alpine evergreen forests, *Remote Sens. Environ.*, *90*, 243–258.

Korner, C. (2000), Biosphere responses to CO_2 enrichment, *Ecol. Appl.*, *10*, 1590–1619.

Krinner, G., et al. (2005), A dynamic global vegetation model for studies of the coupled atmosphere-biosphere system, *Global Biogeochem. Cycles*, *19*(1), GB1015, doi:10.1029/2003GB002199.

Linderholm, H. W. (2006), Growing season changes in the last century, *Agric. For. Meteorol.*, *137*, 1–14.

Lucht, W., et al. (2002), Climatic control of the high-latitude vegetation greening trend and Pinatubo effect, *Science*, *296*, 1687–1689.

McDonald, K. C., J. S. Kimball, E. Njoku, R. Zimmermann, and M. Zhao (2004), Variability in springtime thaw in the terrestrial high latitudes: Monitoring a major control on the biospheric assimilation of atmospheric CO_2 with spaceborne microwave remote sensing, *Earth Interact.*, *8*, 1–23.

Melillo, J. M., et al. (2002), Soil warming and carbon cycle feedbacks to the climate systems, *Science*, *298*, 2173–2176.

Menzel, A., and P. Fabian (1999), Growing season extended in Europe, *Nature*, *397*, 659.

Mitchell, T. D., and P. D. Jones (2005), An improved method of constructing a database of monthly climate observations and associated high-resolution grids, *Int. J. Climatol.*, *25*, 693–712.

Moulin, S., L. Kergoat, N. Viovy, and G. Dedieu (1997), Global-scale assessment of vegetation phenology using NOAA/AVHRR satellite measurements, *J. Clim.*, *10*, 1154–1170.

Myneni, R. B., C. D. Keeling, C. J. Tucker, G. Asrar, and R. R. Nemani (1997), Increased plant growth in the northern high latitudes from 1981 to 1991, *Nature*, *386*, 698–702.

Nemani, R. R., et al. (2003), Climate-driven increases in global terrestrial net primary production from 1982 to 1999, *Science*, *300*, 1560–1563.

Niemand, C., B. Koster, H. Prasse, T. Grunwald, and C. Bernhofer (2005), Relating tree phenology with annual carbon fluxes at Tharandt forest, *Meteorol. Z.*, *14*, 197–202.

Penuelas, J., and I. Filella (2001), Phenology: Responses to a warming world, *Science*, *24*, 793.

Piao, S. L., J. Y. Fang, L. M. Zhou, P. Ciais, and B. Zhu (2006a), Variations in satellite-derived phenology in China's temperate vegetation, *Global Change Biol.*, *12*, 672–685.

Piao, S., P. Friedlingstein, P. Ciais, L. M. Zhou, and A. P. Chen (2006b), The effect of climate and CO_2 changes on the greening of the Northern Hemisphere over the past two decades, *Geophys. Res. Lett.*, *33*, L23402, doi:10.1029/2006GL028205.

Randerson, J. T., C. B. Field, I. Y. Fung, and P. P. Tans (1999), Increases in early season ecosystem uptake explain recent changes in the seasonal cycle of atmospheric CO_2 at high northern latitudes, *Geophys. Res. Lett.*, *26*, 2765–2768.

Reed, B. C., et al. (1994), Measuring phenological variability from satellite imagery, *J. Veg. Sci.*, *5*, 703–714.

Richardson, C. W., and D. A. Wright (1984), A model for generating daily weather variables, technical report, Agric. Res. Serv., U. S. Dep. of Agric., Washington, D. C.

Smith, N. V., S. Saatchi, and J. T. Randerson (2004), Trends in high northern latitude soil freeze and thaw cycles from 1988 to 2002, *J. Geophys. Res.*, *109*, D12101, doi:10.1029/2003JD004472.

Stockfors, J., and S. Linder (1998), The effect of nutrition on the seasonal course of needle respiration in Norway spruce, *Trees*, *12*, 130–138.

Stöckli, R., and P. L. Vidale (2004), European plant phenology and climate as seen in a 20-year AVHRR land-surface parameter dataset, *Int. J. Remote Sens.*, *25*, 3303–3330.

Suzuki, R., T. Nomaki, and T. Yasunari (2003), West-east contrast of phenology and climate in northern Asia revealed using a remotely sensed vegetation index, *Int. J. Remote Sens.*, *47*, 126–138.

Tucker, C. J., D. Slayback, J. E. Pinzon, S. O. Los, R. B. Myneni, and M. G. Taylor (2001), Higher northern latitude normalized difference vegetation index and growing season trends from 1 982 to 1 999, *Int. J. Biometeorol.*, *45*, 184–190.

Tucker, C. J., et al. (2005), An extended AVHRR 8-km NDVI dataset compatible with MODIS and SPOT vegetation NDVI data, *Int. J. Remote Sens.*, *26*, 4485–4498.

Walther, A., and H. W. Linderholm (2006), A comparison of growing season indices for the Greater Baltic Area, *Int. J. Biometeorol.*, *51*, 107–118.

Walther, G. R., et al. (2002), Ecological responses to recent climate change, *Nature*, *416*, 389–395.

Wan, S. Q., Y. Q. Luo, and L. Wallace (2002), Changes in microclimate induced by experimental warming and clipping in tallgrass prairie, *Global Change Biol.*, *8*, 754–768.

Wan, S. Q., D. F. Hui, L. Wallace, and Y. Q. Luo (2005), Direct and indirect effects of experimental warming on ecosystem carbon processes in a tallgrass prairie, *Global Biogeochem. Cycles*, *19*, GB2014, doi:10.1029/2004GB002315.

White, M. A., and R. Nemani (2003), Canopy duration has little influence on annual carbon storage in the deciduous broad leaf forest, *Global Change Biol.*, *9*, 967–972.

White, M. A., S. W. Running, and P. E. Thornton (1999), The impact of growing-season length variability on carbon assimilation and evapotranspiration over 88 years in the eastern US deciduous forest, *Int. J. Biometeorol.*, *42*, 139–145.

Wilson, K. B., and D. D. Baldocchi (2000), Estimating annual net ecosystem exchange of carbon over five years at a deciduous forest in the southern United States, *Agric. For. Meteorol.*, *100*, 1–18.

Zhou, L. M., C. J. Tucker, R. K. Kaufmann, D. Slayback, N. V. Shabanov, and R. B. Myneni (2001), Variations in northern vegetation activity inferred from satellite data of vegetation index during 1981 to 1999, *J. Geophys. Res.*, *106*, 20,069–20,083.

P. Ciais, J. Demarty, P. Friedlingstein, S. Piao, and N. Viovy, Laboratoire des Sciences du Climat et de l'Environnement, CEA/CNRS–LSCE, L'Orme des Merisiers, Bat. 701, F-91191 Gif-sur Yvette Cedex, France. (shilong.piao@lsce.ipsl.fr)